

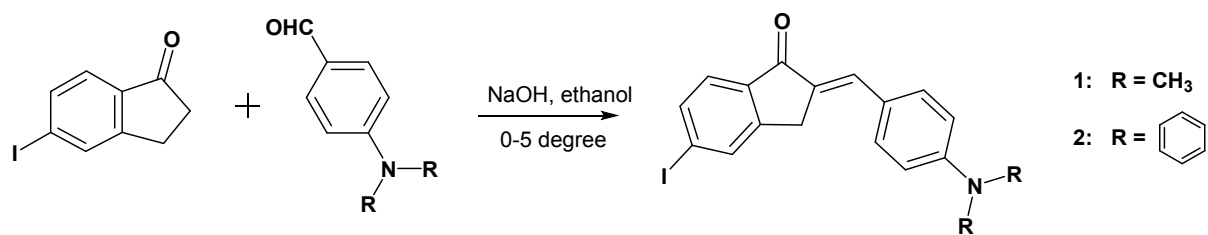
Supporting Information:

**Chalcone single crystals with red emission and photodimerization-triggered hopping behavior: the substituent effect and molecular packing effect**

*Xinrui He, Jian Zhao, Zeqing Tan, Jiaxin Zhao, Xiao Cheng\*, Chuanjian Zhou\**

**Table of Contents**

1. General information	S2-5
2. PXRD of as-synthesized samples	S6-7
3. <sup>1</sup> H-NMR spectra of crystal <b>2</b> before and after UV irradiation.	S8-9
4. Antiparallel molecular stacking structure of crystals <b>1–2</b>	S10
5. Decay curves of <b>1–2</b>	S11-12
6. C-H... $\pi$ interactions in crystal <b>1</b> .	S13
7. Molecular shrinkage in crystal <b>2</b> when excited by UV light	S14
8. Theoretical calculations of molecular interactions	S15-16
9. NMR spectra of compounds <b>1–2</b>	S17-20



**Scheme S1.** Synthetic procedure of compounds **1–2**.

## General Information

**Materials and Instruments.** 5-Iodo-1-indanone (95%), 4-(N,N-Diphenylamino)benzaldehyde (98%) and 4-Dimethylaminobenzaldehyde (99%) were obtained from J&K Scientific, all the other ingredients were obtained from J&K Scientific or Aladdin, and were used without further purification. NMR spectra were recorded on a Bruker Avance 500 MHz spectrometer with tetramethylsilane as the internal standard, while mass spectra were recorded on an Agilent Q-TOF 6510 mass spectrometer. Elemental analyses were performed on an Elementar Vario EL Cube spectrometer. UV-vis absorption spectra were recorded on a Shimadzu UV-2600 spectrophotometer. Emission spectra were recorded using a Shimadzu RF-6000 spectro fluorophotometer. Lifetimes were measured on an Edinburgh FLS920 spectrometer. Microscopy images and crystal jumping videos were measured on an OLYMPUS BX51 fluorescence microscope with a 100 W mercury light source. Powder X-ray diffraction (PXRD) patterns were acquired on a Bruker D8 advance powder X-ray Cu Ka radiation diffractometer. All measurements were carried out at room temperature under ambient conditions.

**Synthetic procedure.** The synthetic route of compounds **1–2** is shown in Scheme S1. Two reactants, 5-Iodo-1-indanone (2.58 g, 10 mmol) and benzaldehyde derivative (1.49g 4-Dimethylaminobenzaldehyde for compound **1**, 2.73g 4-(N,N-Diphenylamino)benzaldehyde for compound **2**, 10 mmol), were dissolved in 60 mL ethanol at zero degrees centigrade. Aqueous NaOH (1.0 g in 2 ml H<sub>2</sub>O) was added to the mixture drop by drop. Then, the mixture

was stirred for 3 h at zero degrees Celsius. The precipitates were filtered out, washed with water and cold ethanol, and then dried as crude product. The crude product was recrystallized twice in CH<sub>2</sub>Cl<sub>2</sub>/ethanol mixture to obtain large amount of yellow/red crystals or crystalline solids. Compounds **1–2** were characterized by NMR, mass spectra, elemental analysis and single crystal X-ray diffractions.

(2*E*)-5-iodo-2-[[4-(dimethylamino)phenyl]methylene]-2,3-dihydro-1*H*-inden-1-one (**1**).

Yield: 76%. <sup>1</sup>H NMR (500 MHz, CDCl<sub>3</sub>):  $\delta$  7.74(d, *J* = 8.00 Hz, 1H), 7.70 (s, 1H), 7.65 (s, 1H), 7.58 (d, *J* = 9.00 Hz, 2H), 7.54 (d, *J* = 9.50 Hz, 1H), 6.81 (d, *J* = 8.00 Hz, 2H), 3.96 (s, 2H), 3.07 (s, 6H). <sup>13</sup>C NMR (125 MHz, CDCl<sub>3</sub>):  $\delta$  193.03, 151.20, 150.97, 137.65, 135.70, 132.89, 130.90, 129.21, 128.98, 128.68, 125.26, 122.92, 111.95, 40.08, 32.40. MS *m/z*: 390.03 [M]<sup>+</sup> (calcd: 389.03). Anal. Calcd (%) for C<sub>18</sub>H<sub>16</sub>INO: C, 55.54; H, 4.14; N, 3.60. Found: C, 55.58; H, 4.31; N, 3.55.

(2*E*)-5-iodo-2-[[4-(diphenylamino)phenyl]methylene]-2,3-dihydro-1*H*-inden-1-one (**2**). Yield: 72%. <sup>1</sup>H NMR (500 MHz, CDCl<sub>3</sub>):  $\delta$  7.94 (s, 1H), 7.78 (d, *J* = 8.00 Hz, 1H), 7.64 (s, 1H), 7.61 (d, *J* = 8.00 Hz, 1H), 7.51 (d, *J* = 8.50 Hz, 2H), 7.32 (t, *J* = 8.00 Hz, 4H), 7.17 (m, 6H), 7.06 (d, *J* = 8.50 Hz, 2H), 3.96 (s, 2H). <sup>13</sup>C NMR (500 MHz, CDCl<sub>3</sub>):  $\delta$  193.40, 150.92, 149.61, 146.69, 137.89, 136.99, 135.46, 134.74, 132.21, 131.13, 129.60, 127.93, 125.69, 125.42, 124.37, 121.27, 102.23, 32.13. MS *m/z*: 514.05 [M]<sup>+</sup> (calcd: 513.06). Anal. Calcd (%) for C<sub>28</sub>H<sub>20</sub>INO: C, 65.51; H, 3.93; N, 2.73. Found: C, 64.90; H, 3.95; N, 2.56.

### Single-crystal X-ray Diffraction.

Single-crystal X-ray diffraction data were collected on a Oxford (Varian) Gemini A Ultra diffractometer in  $\omega$ -scan mode using graphite-monochromated Mo-K $\alpha$  radiation. Structures were solved with direct methods using the SHELXTL program and refined with full-matrix least squares on *F*<sup>2</sup>. Non-hydrogen atoms were refined anisotropically, while the positions of hydrogen atoms were calculated and refined isotropically. [CCDC 1975884 for **1** and 1975885 for **2** contain the supplementary crystallographic data for this paper. These data can

be obtained free of charge from The Cambridge Crystallographic Data Centre via [www.ccdc.cam.ac.uk/data\\_request/cif](http://www.ccdc.cam.ac.uk/data_request/cif).]

### **Calculations.**

All the geometries are based on the experimentally-obtained single crystal data whose optimizations were performed from ORCA 4.1.0 <sup>[1,2]</sup> at B3LYP-D3(BJ)/def2-SVP level of theory <sup>[3]</sup>. At the same level, the frequency was calculated to guarantee that the geometry is located on the true minima on the potential energy surfaces. The electronic energy was calculated at the B3LYP-D3(BJ)/def2-TZVPD, and The Boys and Bernardi's counterpoise (CP) technique <sup>[4]</sup> was introduced to correct the problem of basis set superposition error (BSSE). The HOMO and LUMO orbitals were plotted by VMD 1.93 <sup>[5]</sup> whose input files were extracted from Multiwfn 3.7 <sup>[6]</sup>. Noncovalent interactions which are in a wide range of attraction and repulsion forces between atoms or molecules were visualized from NCI analysis<sup>[7]</sup>.

### **References**

- [1] Neese, F. The ORCA program system Wiley Interdisciplinary Reviews: Computational Molecular Science, 2012, 2(1): 73-78.
- [2] Neese, F. Software update: the ORCA program system, version 4.0 Wiley Interdisciplinary Reviews:Computational Molecular Science, 2017, 8(1): e1327.
- [3] Goerigk, L., Grimme, S. Efficient and Accurate Double-Hybrid-Meta-GGA Density Functionals Evaluation with the Extended GMTKN30 Database for General Main Group Thermochemistry, Kinetics, and Noncovalent Interactions. Journal of chemical theory and computation, 2010, 7(2): 291-309.
- [4] Boys, S. F., Bernardi, F. D. The calculation of small molecular interactions by the differences of separate total energies. Some procedures with reduced errors. Molecular Physics, 1970, 19(4): 553-566.

- [5] Humphrey, W., Dalke, A., Schulten, K. VMD: visual molecular dynamics. *Journal of molecular graphics*, 1996; 14(1): 33-38.
- [6] Lu, T., Chen, F. Multiwfn: a multifunctional wavefunction analyzer. *Journal of computational chemistry*, 2012, 33(5): 580-592.
- [7] Johnson, E. R., Keinan, S., Mori-Sánchez, P., Contreras-García, J., Cohen, A. J., Yang, W. (2010). Revealing noncovalent interactions. *Journal of the American Chemical Society*, 132(18): 6498-6506.

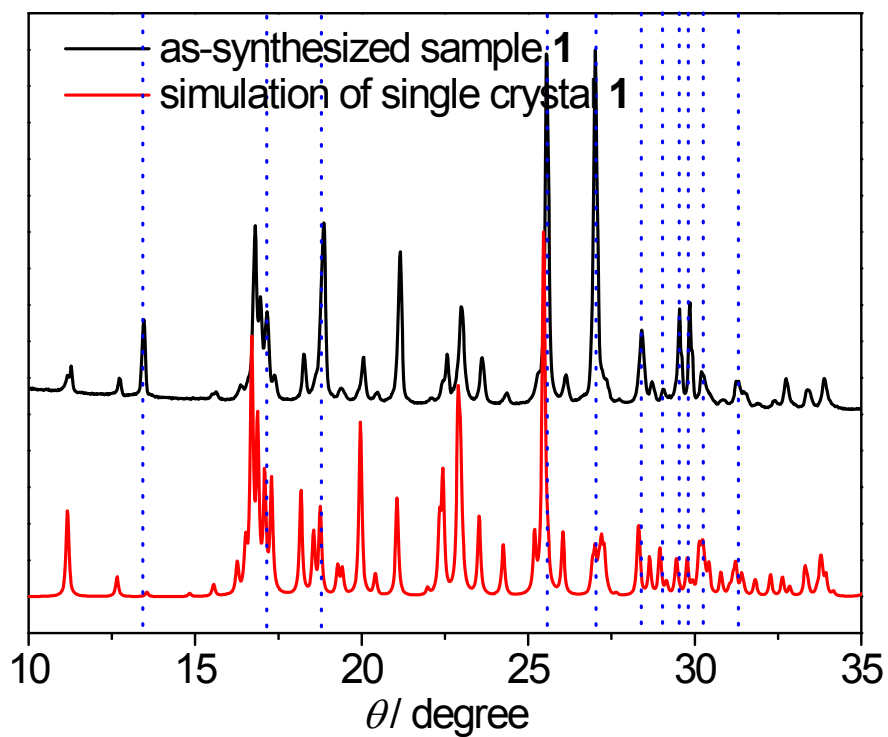


**Figure S1.** Powder X-ray diffraction pattern of as-synthesized sample **1** and simulation of single crystal **1**.

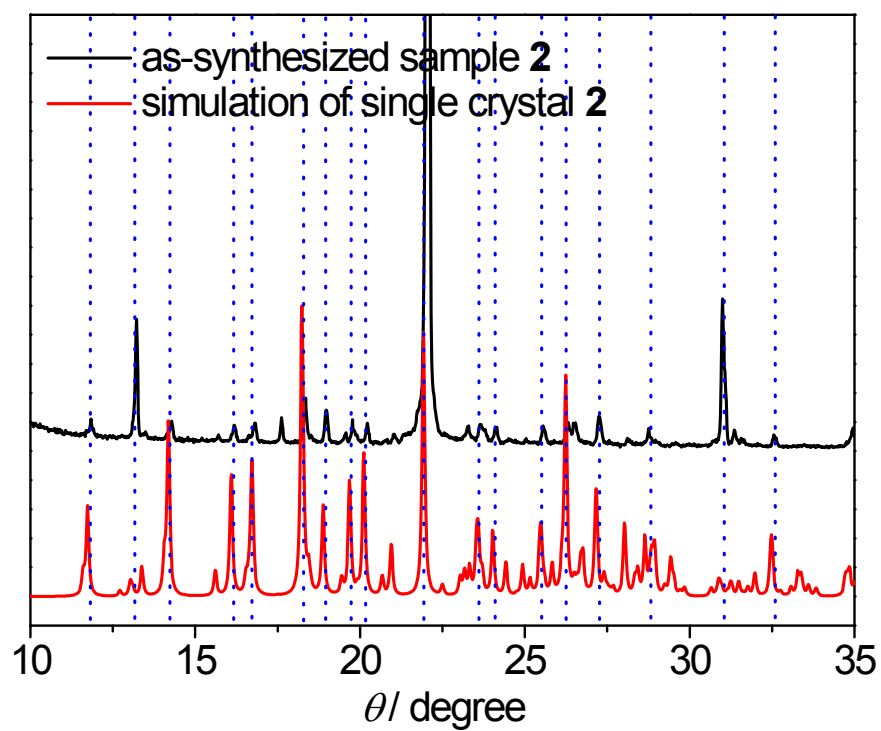


**Figure S2.** Powder X-ray diffraction pattern of as-synthesized sample **2** and simulation of single crystal **2**.

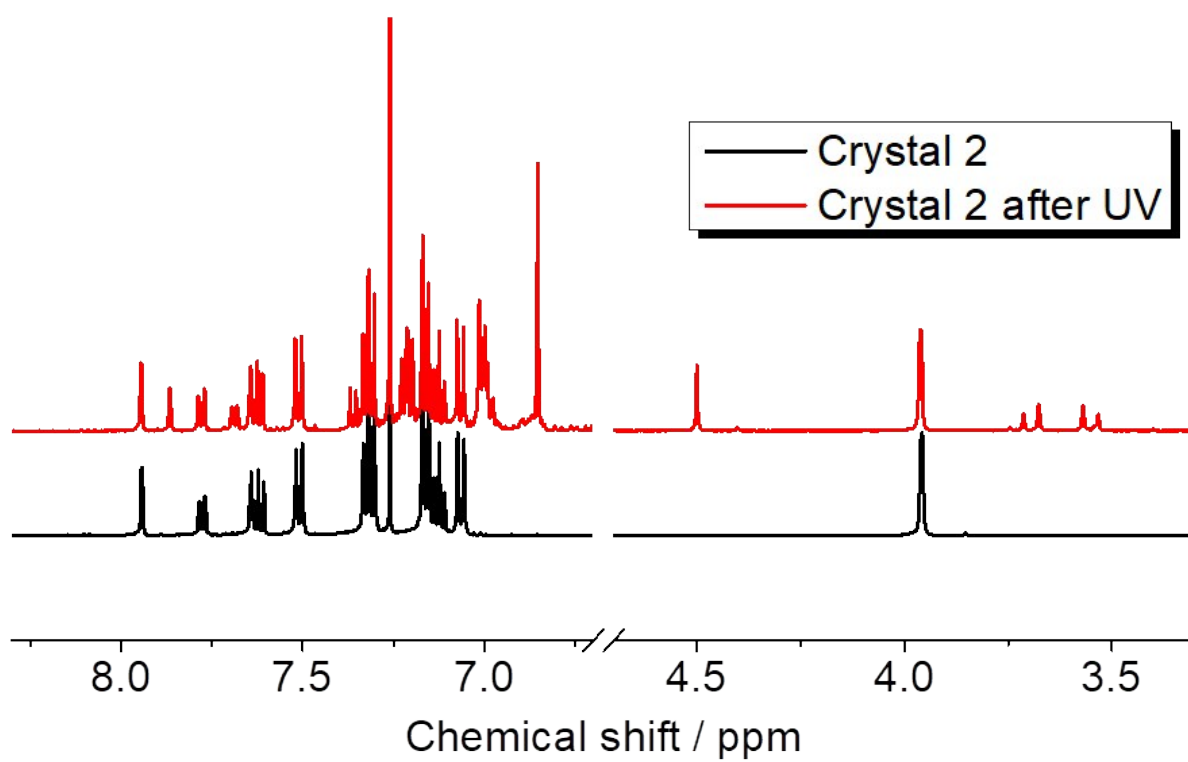


**Figure S3.**  $^1\text{H}$  NMR spectra for crystal **2** before and after UV irradiation.



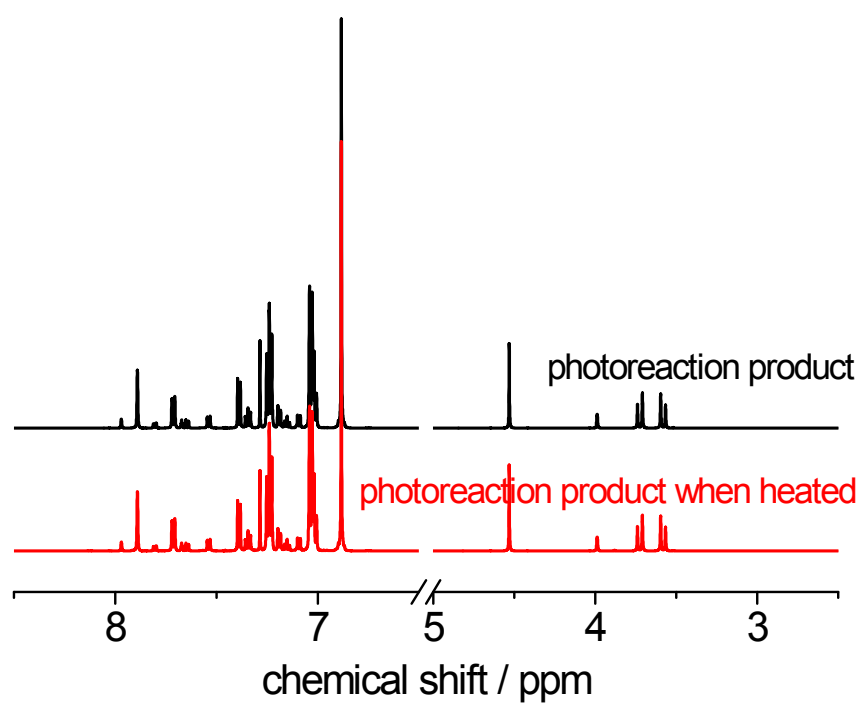


**Figure S4.** Comparison of the  $^1\text{H}$  NMR spectra for the photoreaction product before and after heating process.

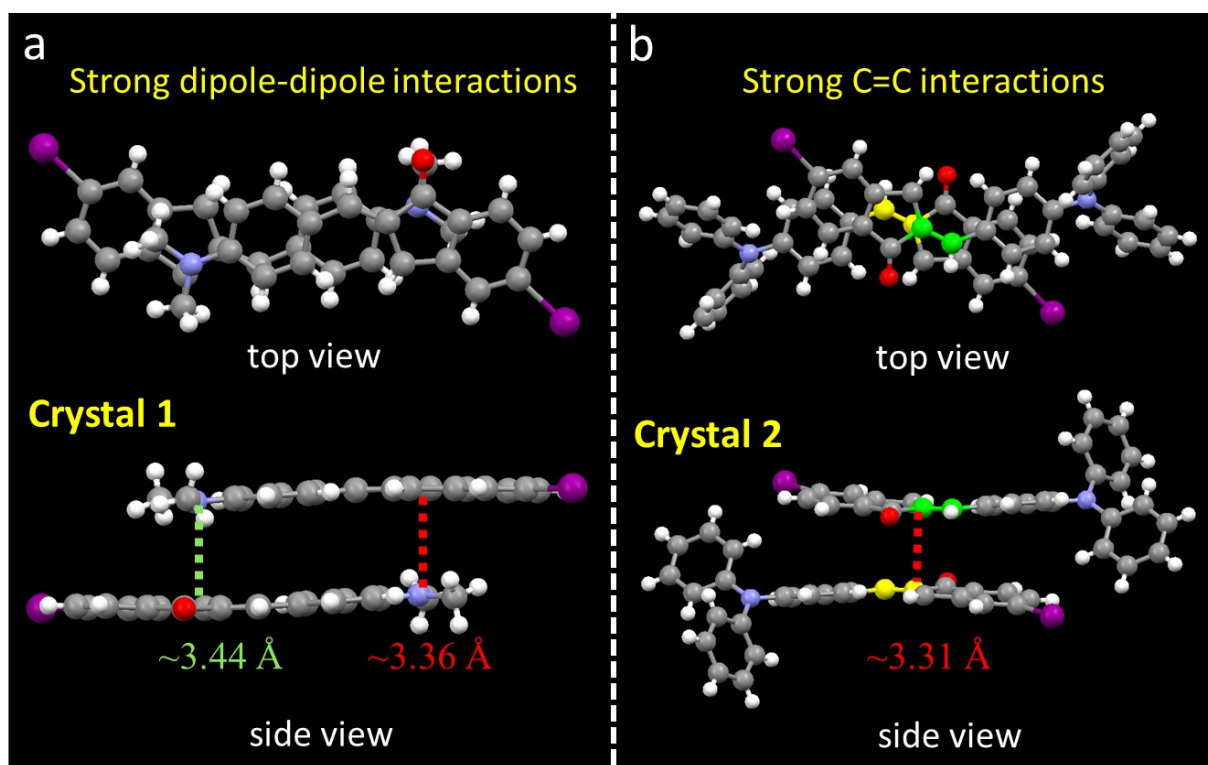


**Figure S5.** Antiparallel molecular stacking structure of crystal **1** with strong dipole-dipole interactions and crystal **2** with strong C=C interactions.

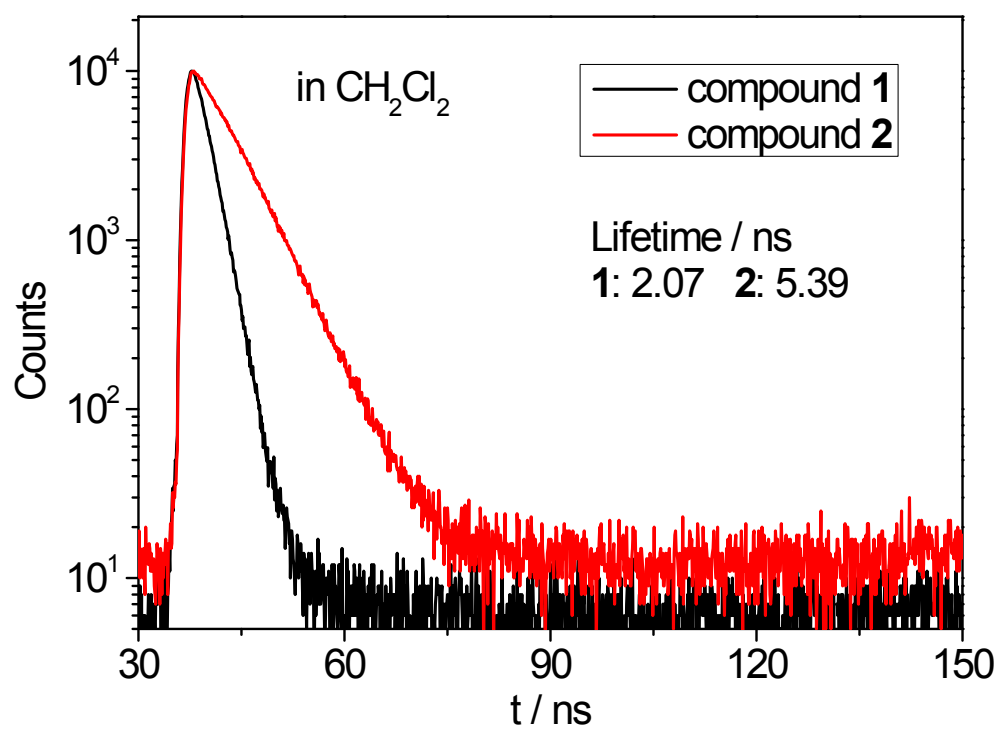


**Figure S6.** Decay curves of compounds **1–2** in CH<sub>2</sub>Cl<sub>2</sub>.

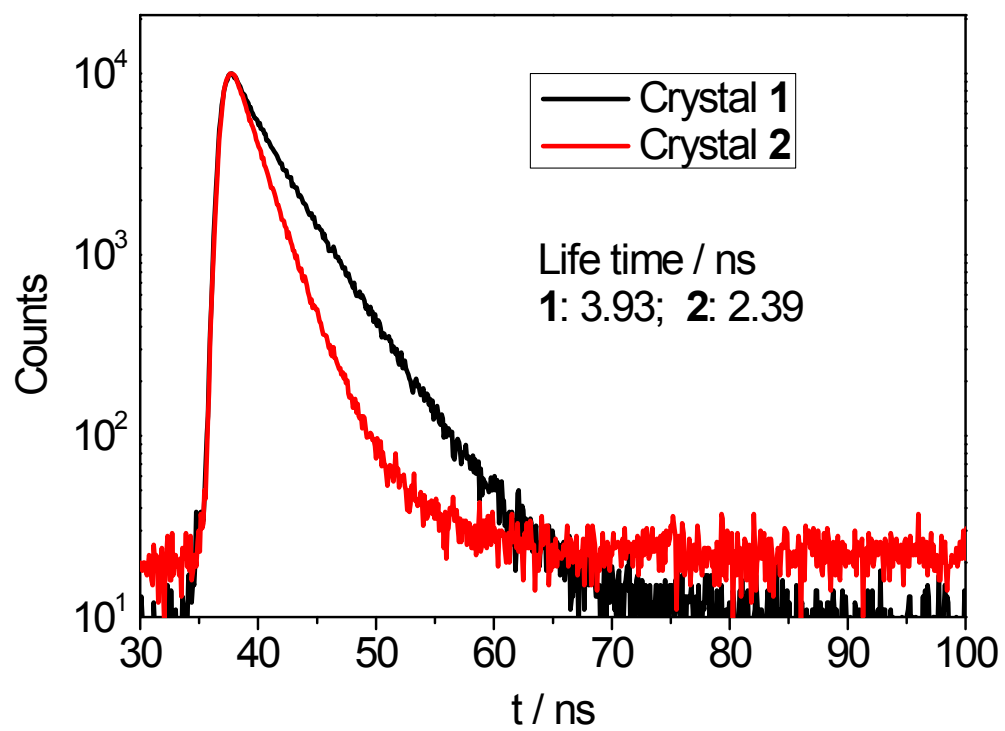


**Figure S7.** Decay curves of crystals 1–2.

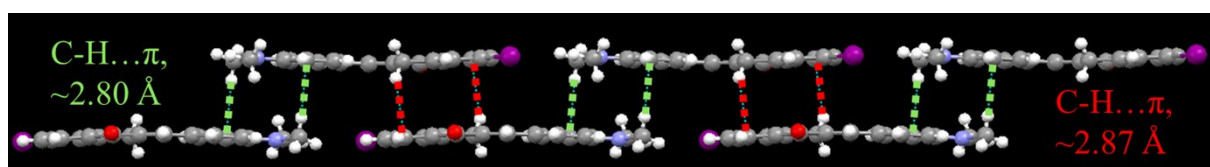


**Figure S8.** C-H... $\pi$  interactions in one direction of crystal **1**.

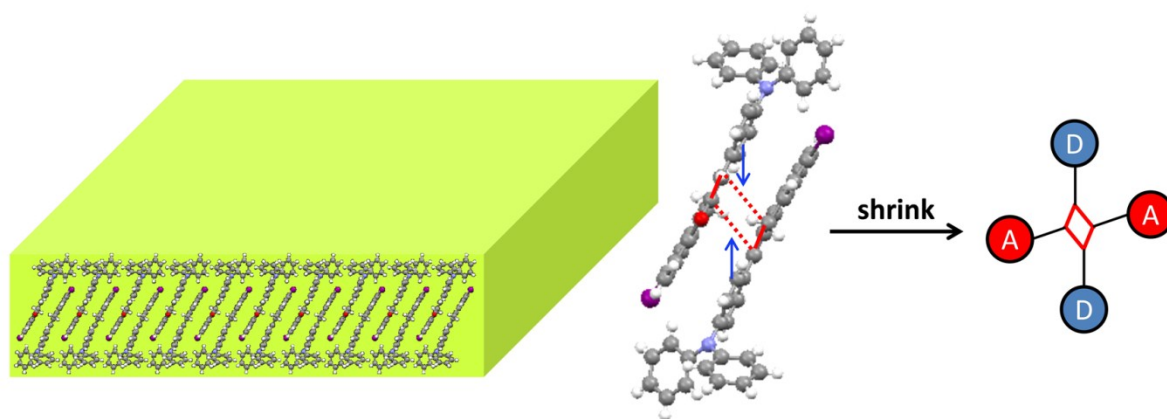


**Figure S9.** Schematic diagram featuring molecular shrinkage in crystal **2** when photodimerization take place (A = acceptor, D = donor).

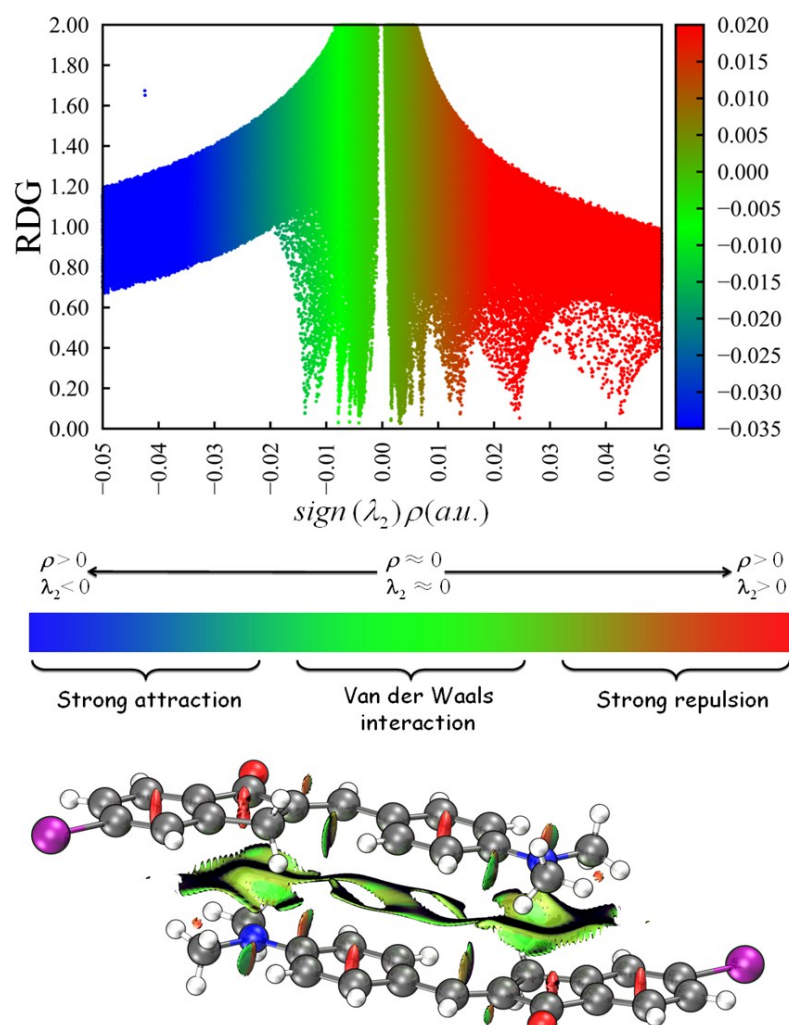


**Figure S10.** The RDG isosurfaces as well as color-filled map of RDG versus the product of second Hessian eigen and electron density for compound **1** when stack in molecular pairs. The  $\text{sign}(\lambda_2)\rho$  is mapped on the isosurface of RDG, where the values of  $\text{sign}(\lambda_2)\rho$  are in the range of -0.035~0.020 with the different colors from blue to red.

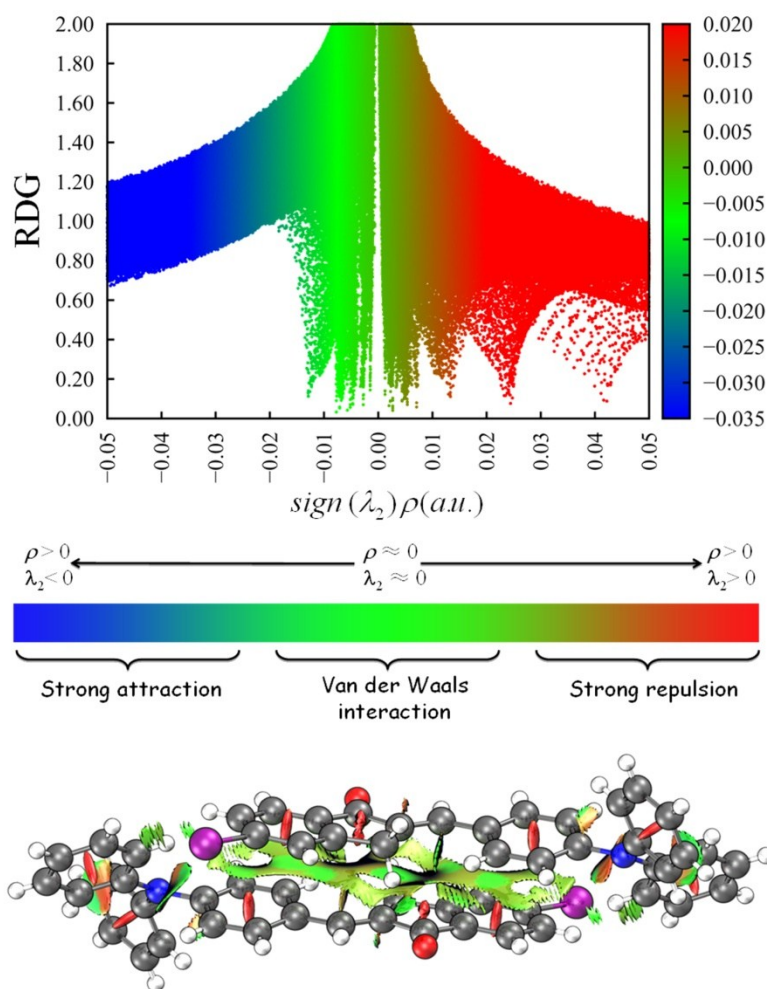


**Figure S11.** The RDG isosurfaces as well as color-filled map of RDG versus the product of second Hessian eigen and electron density for compound **2** when stack in molecular pairs. The  $\text{sign}(\lambda_2)\rho$  is mapped on the isosurface of RDG, where the values of  $\text{sign}(\lambda_2)\rho$  are in the range of -0.035~0.020 with the different colors from blue to red.



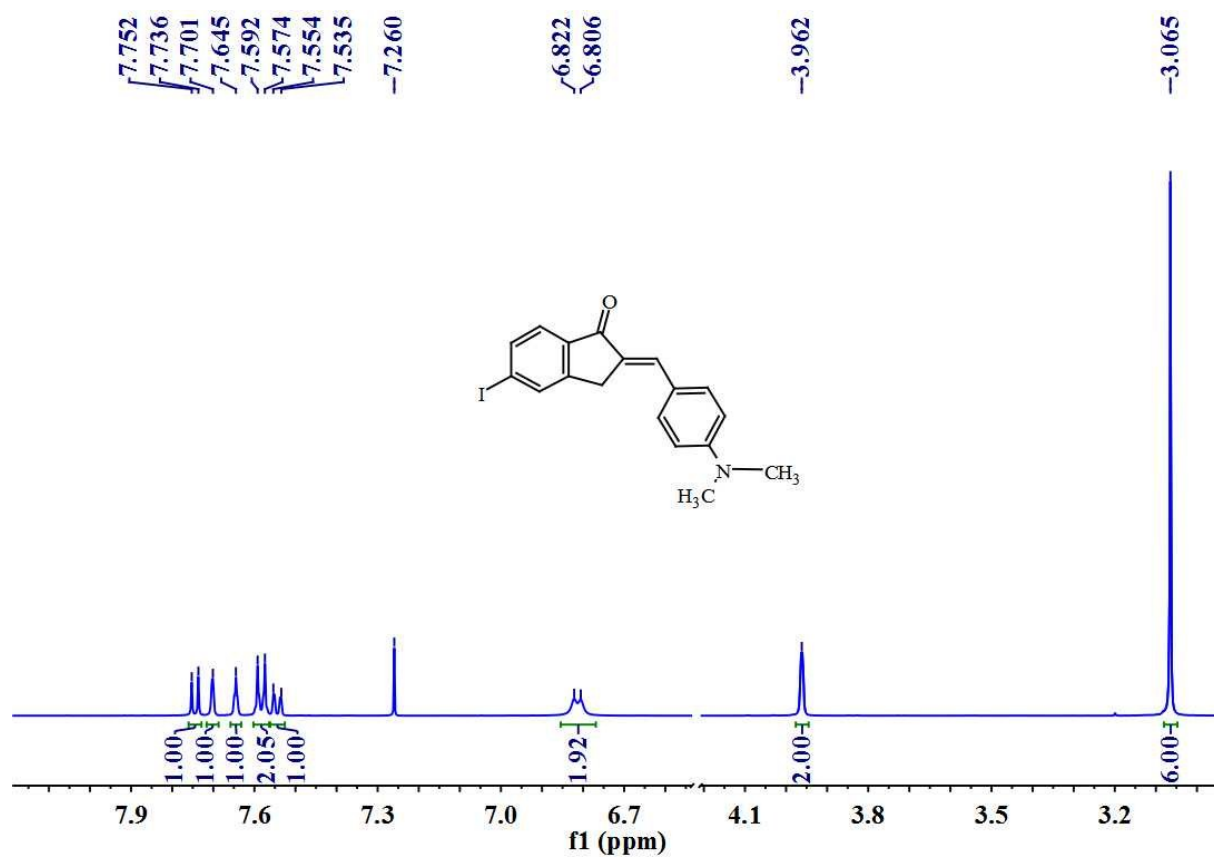


**Figure S12.** <sup>1</sup>H NMR spectra for compound **1** in CDCl<sub>3</sub> (500 MHz).

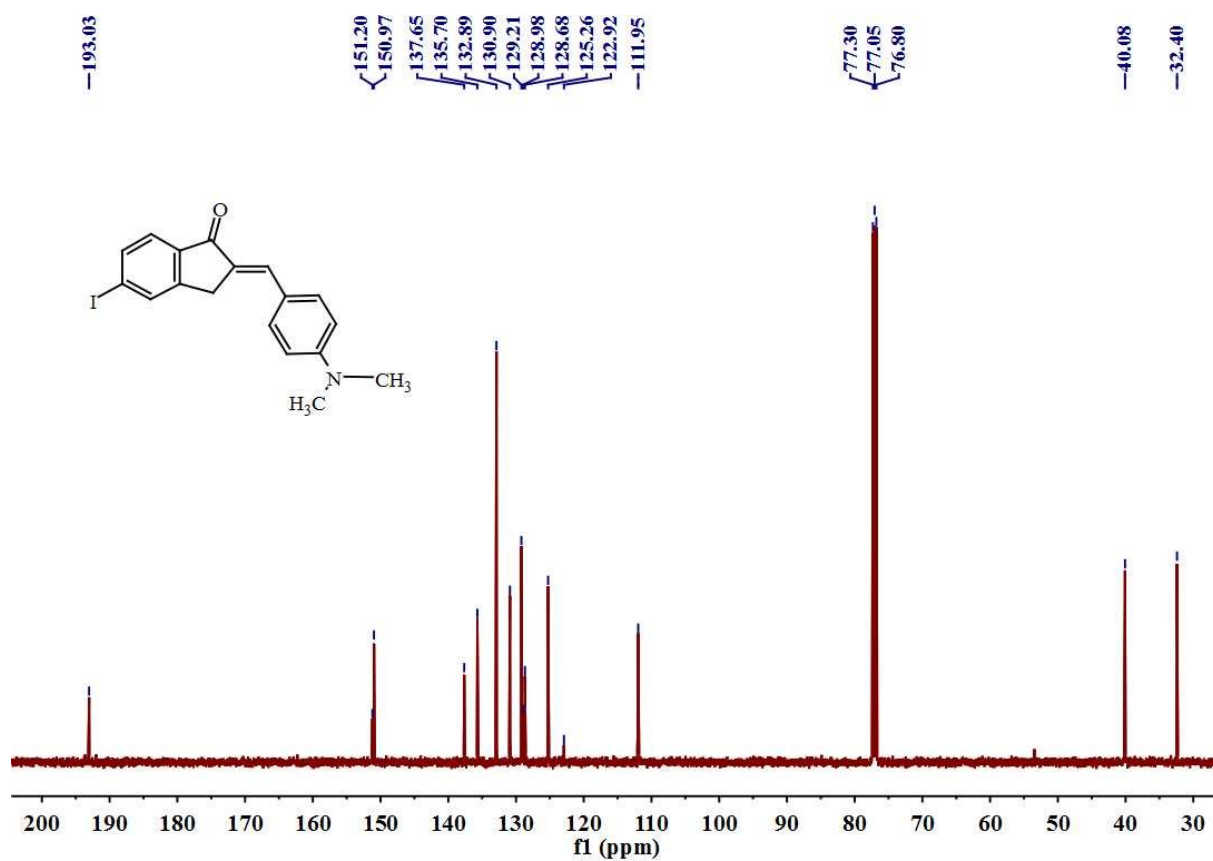


**Figure S13.** <sup>13</sup>C NMR spectrum of compound **1** (125 MHz, CDCl<sub>3</sub>).

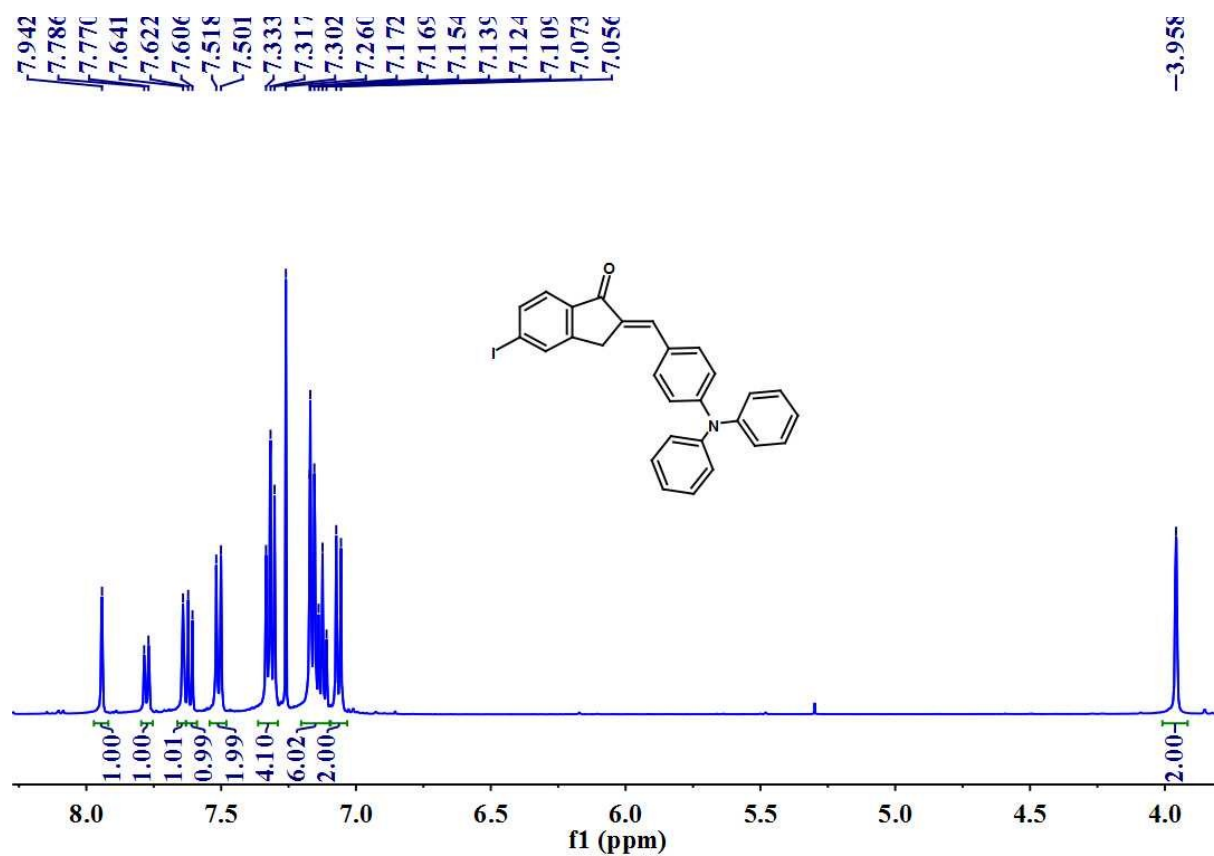


**Figure S14.**  $^1\text{H}$  NMR spectrum for compound **2** in  $\text{CDCl}_3$  (500 MHz).

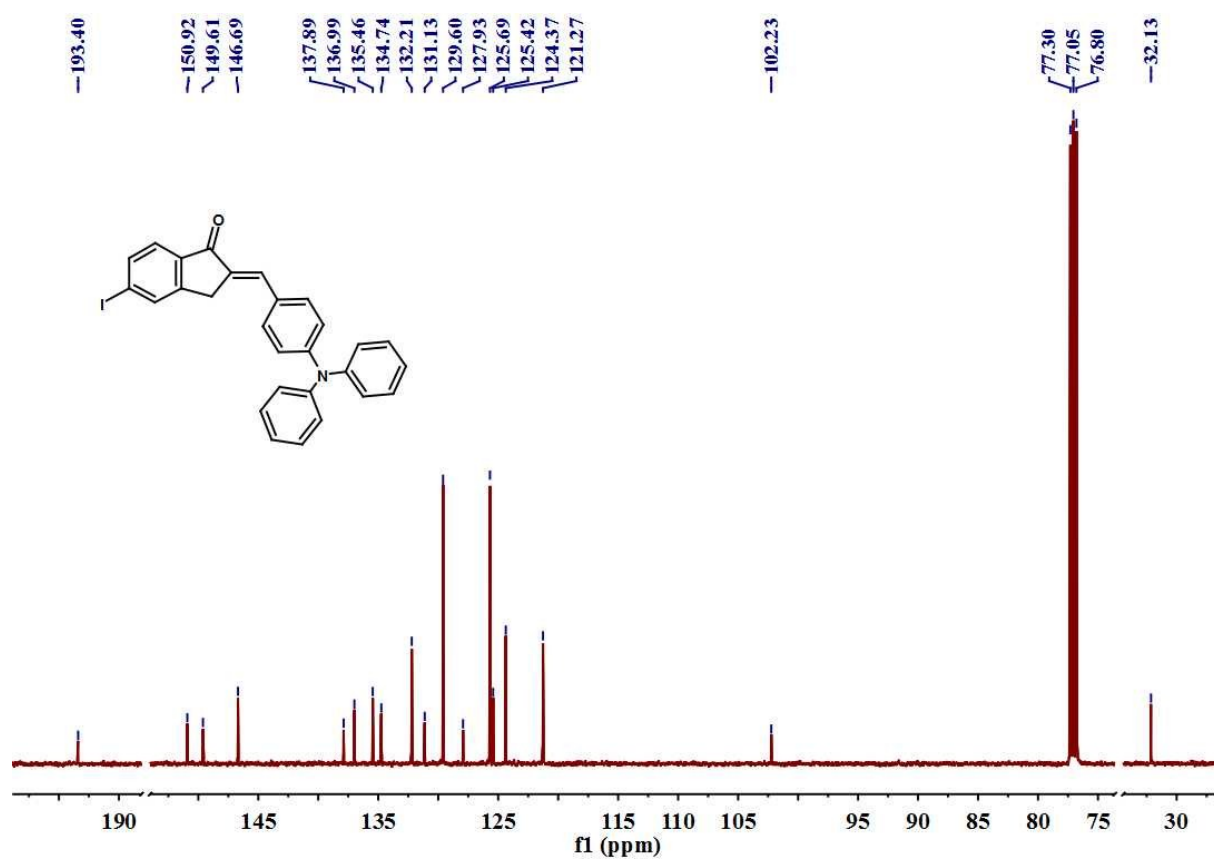


**Figure S15.** <sup>13</sup>C NMR spectrum of compound **2** (125 MHz, CDCl<sub>3</sub>).